Catal Lett
DOI 10.1007/s10562-015-1537-0

Highly Uniform Pd Nanoparticles Supported on g-C_3N_4 for Efficiently Catalytic Suzuki–Miyaura Reactions

Xiangyang Su[1] · Ajayan Vinu[2] · Salem S. Aldeyab[3] · Lin Zhong[1]

Received: 26 February 2015 / Accepted: 19 April 2015

Abstract Pd nanoparticles were supported on the surface of g-C_3N_4 by a facile method assisted by ultrasonication. The Pd/g-C_3N_4 catalyst was characterized by N_2-adsorption, X-ray diffraction (XRD), transmission electron microscopy (TEM), and X-ray photoelectron spectroscopy (XPS). The XRD and TEM analyses reveal that the Pd nanoparticles are evenly distributed on the surface of g-C_3N_4 with an average size of 4 nm. The XPS results indicate that the Pd interacts with the N of g-C_3N_4. The supported catalyst shows high efficiencies in Suzuki–Miyaura reactions with up to 99 % isolated yield under mild reaction conditions. The catalyst can be easily recycled at least 3 times without any loss of activity and selectivity. The excellent performance of the catalyst in activity and reusability may be attributed to the strong interaction between g-C_3N_4 and Pd nanoparticles, and the robust nature of the CN framework, respectively.
Graphical Abstract

Electronic supplementary material The online version of this article (doi:10.1007/s10562-015-1537-0) contains supplementary material, which is available to authorized users.

✉ Lin Zhong
zhonglin@scu.edu.cn

[1] College of Chemical Engineering, Sichuan University, Chengdu 610065, Sichuan, China

[2] Australian Institute for Bioengineering and Nanotechnology, University of Queensland, Brisbane, QLD 4072, Australia

[3] Petrochemical Research Chair, Department of Chemistry, King Saud University, Riyadh, Saudi Arabia

Published online: 28 April 2015

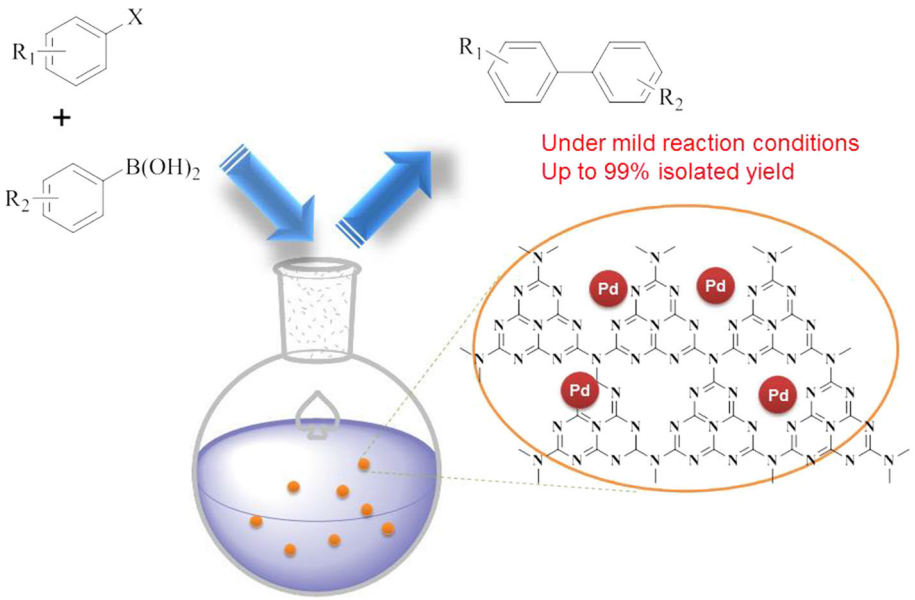

Keywords Pd nanoparticles · g-C_3N_4 · Suzuki–Miyaura reaction · Heterogeneous catalysis

1 Introduction

The Suzuki–Miyaura reaction is one of the most important organic transformations for constructing carbon–carbon bond [1]. Over the decades, the Suzuki–Miyaura reaction with Pd-based catalyst has achieved great progress and been applied extensively in polymer science and fine chemicals and pharmaceutical industries [2, 3]. However, the reaction is still facing some challenges such as difficulty in separating the product and recycling high-cost Pd species [4, 5]. Heterogenization of Pd-based catalyst can provide a simple but efficient method to overcome the drawback though the activity in heterogeneous system is usually lower than that of homogeneous competitor [6–8]. Recently, supported Pd nanoparticles have demonstrated the capacity of catalyzing the Suzuki–Miyaura reaction which aroused great interest from the industry [9, 10]. However, the development of novel supported Pd catalyst with a high activity and reusability remains very challenging and timely [11–17]. The so-called g-C_3N_4 which is the most stable allotrope of carbon nitride has generated widespread attention for its applications in materials science and catalysis [18]. For example, the recent researches have shown that g-C_3N_4 is a unique support for metal nanocatalysts with excellent catalytic performance [19, 20]. Nevertheless, the work involving Pd nanoparticles supported on g-C_3N_4 for Suzuki–Miyaura reaction is very rare [21, 22]. Li and Antonietti et al. firstly reported the Suzuki coupling reaction over the supported Pd catalysts on the surface of g-C_3N_4 by light-mediated catalyst activation. They found that under photo irradiation and very mild conditions, the stimulated electron transfer from g-C_3N_4 nanorods to Pd nanoparticles plays an important role in activating the substrates of the Suzuki coupling reactions with a high activity and selectivity [21]. Very recently, Fu and Wang et al. developed a photodeposition method to prepare uniformly dispersed Pd nanoparticles on g-C_3N_4 [22]. The nanocomposite shows superior catalytic activity in the Suzuki–Miyaura coupling reactions. However, the activity of the catalyst decreased remarkably from 100 % to about 85 % after three recycles [22]. Although no explanation for the activity decrease was presented in the paper, it is believed that the declined activity may be due to the week interaction between Pd nanoparticles and g-C_3N_4 as the photoreduction method used in this process to support metal nanoparticles normally results in moderate or even weedy metal-support interaction [23]. Herein, we prepared the Pd nanoparticles supported on g-C_3N_4 by a facile ultrasonic-assisted solution reduction method. It was found that the supported catalyst exhibits a high activity and selectivity in the Suzuki–Miyaura reaction under mild reaction conditions. Moreover, the catalyst can be straightforwardly reused for at least three times without any loss of activity and selectivity. The strong interaction between the Pd nanoparticles and the g-C_3N_4 support may be attributed for the outstanding performance and the stability of the catalyst.

2 Experimental

2.1 Catalyst Preparation

The g-C_3N_4 was synthesized using urea as carbon and nitrogen source and SiO_2 nanosphere as a hard template [24]. Briefly, 5 g of 40 % SiO_2 solution (Ludox HS40, 12 nm) was added into 10 g of urea solution and then the mixture was heated at 90 °C under stirring. After the evaporation of water, a white solid was collected and then carefully grinded. Then, the power was transferred into a covered quartz boat and heated to 550 °C in a tubular furnace at a heating rate of 3 K min^{-1} in air. The heating at 550 °C was retained for 4 h to complete the polymerization of urea. A yellow solid was gathered and put into a 2 M NaOH solution to remove the SiO_2 template at room temperature. After 24 h, a light yellow solid was filtered and washed with water and ethanol several times. Finally, the obtained g-C_3N_4 was dried at 70 °C in a vacuum oven overnight.

The supported Pd catalyst was synthesized by an ultrasonic-assisted solution method [25]. 0.2 g g-C_3N_4 was dispersed into 20 ml water and ultrasonicated for 15 min. Then, 4 ml $PdCl_2$ (1 % w/w) solution was added into the mixture. After further ultrasonication for another 15 min. 10 ml $NaBH_4$ solution was added into the mixture to reduce the Pd(II) to Pd(0). After filtration, the black solid was washed with water and ethanol fully. Then, the catalyst was dried at 70 °C in a vacuum oven overnight.

2.2 Materials and Characterization

LUDOX HS-40 colloidal silica was obtained from Sigma Aldrich. 2-Bromotoluene (98 %), 4-bromoanisole (97 %), 4-bromobenzaldehyde (95 %) and 4-methoxyphenylboronic acid were purchased from J&K Scientific Ltd. Iodobenzene (99 %) and bromobenzene (99 %) were delivered by Chengdu Best Reagent Co., Ltd. Urea, $PdCl_2$ (59 %), phenylboronic acid (98 %) and chlorobenzene (99 %) were provided by Chengdu Kelong Chemical Co., Ltd. All the chemicals are commercially available and were used as-received.

The N_2 adsorption–desorption isotherms and pore diameter distribution were measured by Quantachrome Instruments Quadrasorb-SI. Scanning electron microscope (SEM) was conducted on JEOL JSM-7500F. The transmission electron microscopy (TEM) was performed on Tecnai G2 F20 S-TWIN at an acceleration voltage of 200 kV. Samples for TEM measurement were prepared by placing a small drop of a colloid suspension in ethanol on a carbon-coated copper grid. X-ray diffraction (XRD) data was collected on Philips X'Pert MPD diffractometer at a scanning rate of 0.03° s^{-1} in the 2θ range from 10° to 80°. The X-ray photoelectron spectroscopy (XPS) was recorded on Kratos XSAM800 (Al Kα, 1486.69 eV) and the charging effect was corrected by the C1 s peak at 284.6 eV. The Pd loading of the catalysts was determined by SPECTRO ARCOS inductively coupled plasma atomic emission spectroscopy (ICP-AES). Proton nuclear magnetic resonance (^{1}H NMR) was carried out on Bruker 400 MHz NMR spectrometer to confirm the structure of the Suzuki–Miyaura reaction products.

2.3 Catalytic tests

For a typical reaction, the mixture of bromobenzene (0.5 mmol, 78.5 mg), phenylboronic acid (0.55 mmol, 61 mg) and 4 mg catalyst was added into a pressure-resisting reaction flask. The flask was sealed after the addition of K_2CO_3 (2 mmol, 276 mg) and 4 ml H_2O–ethanol (v/v = 1:1). The reaction was then carried out at 80 °C for 2 h. After the substrate bromobenzene was converted completely (monitored by the TLC analysis), the catalyst was separated by a short column (silica gel). The product was purified by column chromatography (silica gel, petroleum ether/acetic ether). The structures of the products were further confirmed by ^{1}H NMR.

2.4 Catalyst Recycling Experiment

4-Bromoanisole (0.5 mmol, 93.5 mg) and phenylboronic acid (0.55 mmol, 61 mg) and 4 mg catalyst were added into a pressure-resisting reaction flask, followed by the addition of K_2CO_3 (276 mg, 2 mmol) and 4 ml H_2O–ethanol (v/v = 1:1). The reaction flask was then sealed and heated at 80 °C for 2.5 h. Then, the reaction mixture was cooled to room temperature and transferred into a centrifuge tub. After centrifuged at 5000 rpm for 15 min, the supernatant in the tube was carefully removed and the remaining solid was washed with water and ethanol. The procedure of centrifuge and washing were repeated three times. The separated catalyst was then used for the next reaction cycle.

3 Results and Discussion

Nitrogen adsorption–desorption experiments were performed on g-C_3N_4 and Pd/g-C_3N_4 (Table 1; Fig. 1). All samples showed a type IV/H3 adsorption isotherms which indicated the existence of mesopores in the samples. For g-C_3N_4, which was synthesized by a template method [24], the templating effect is surprisingly limited. Most of the pore sizes in g-C_3N_4 are concentrated at about 5.6 nm instead of 12 nm, the particle size of the silica template. However, the g-C_3N_4 yield (8 wt%) is about twice that of

Table 1 Textural properties of g-C_3N_4 and Pd/g-C_3N_4

Sample	BET surface area (m^2 g^{-1})	Pore volume (cm^3 g^{-1})	Pore size (nm)
g-C_3N_4	17	0.10	5.6
Pd/g-C_3N_4	30	0.13	5.6

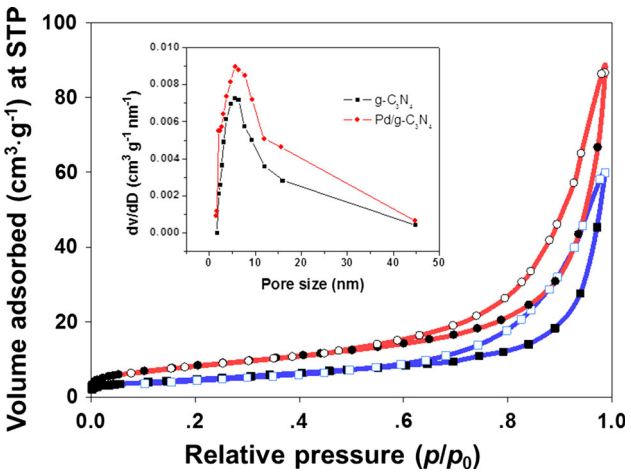

Fig. 1 N_2 adsorption–desorption isotherms of g-C_3N_4 (○ and ●) and Pd/g-C_3N_4 (□ and ■) (Inset: Barrett−Joyner−Halenda (BJH) pore size distribution profiles)

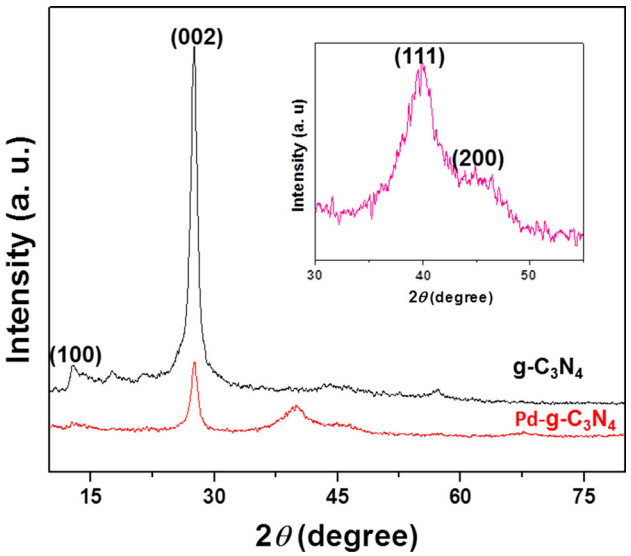

Fig. 2 XRD profiles of g-C_3N_4 and Pd/g-C_3N_4

the one prepared without template [26]. After supporting Pd nanoparticles (the Pd loading determined by ICP is 14 wt%), the pore size destitution and pore volume of the g-C_3N_4 are nearly retained, revealing that Pd nanoparticles are mostly dispersed on the outside of the pores. The minimal change in the nitrogen adsorption–desorption isotherms of the g-C_3N_4 further reveal that the pores of the g-C_3N_4 are not altered by the supported Pd nanoparticles. Interestingly, compared with the support, the surface area of the catalyst Pd/g-C_3N_4 increases slightly from 17 to 30 m^2 g^{-1}. The increase may due to ultrasonic effect which could exfoliate the g-C_3N_4 resulting in higher surface area during the synthesis of the catalyst [27].

The XRD patterns of the g-C_3N_4 and Pd/g-C_3N_4 are shown in Fig. 2. Before the Pd deposition, there are two prominent peaks for g-C_3N_4: the strong peak (002) at 27.6° relates to the inter-planar stacking structure of g-C_3N_4, while the weak (100) peak at 13.3° is derived the lattice planes parallel to the *c*-axis [26–28]. However, after the Pd deposition, two broadly peaks appear at 40.0° and 46.2° which are assigned to the (111) and (200) planes of Pd(0) respectively [19, 29]. The average size of the Pd nanoparticles determined by Scherrer's equation with measuring the half width of the (111) peak is about 3.7 nm.

The morphology of g-C_3N_4 before and after Pd deposition was then investigated by means of SEM and TEM. As shown in Fig. 3a, b, g-C_3N_4 was formed with typically layered platelet-like morphology. This layered structure may generate mesopores in g-C_3N_4 which are available sites for adsorption of nitrogen during nitrogen adsorption–desorption experiments. The TEM images of Pd/g-C_3N_4 (Fig. 3c, d clearly demonstrated that the small-sized Pd particles are evenly distributed on the surface of g-C_3N_4 after the deposition. The average size of the nanoparticles is about 3.9 nm which is well consistent with the value determined by XRD. Figure 3e shows the Pd crystal planes measured as 0.226 nm which is attributed to the lattice spacing of (111) plane of metallic Pd [19, 25]. Thus, these results revealed that highly uniform Pd nanoparticles can be supported successfully on g-C_3N_4 by the ultrasonic-assisted method. Moreover, the strong interactions between Pd nanoparticles and the π bonded planar -layers and incompletely condensed amino groups of g-C_3N_4 could induce the formation small-sized Pd nanoparticle and then stabilize the resulted nanoparticles [19].

XPS tests were carried out to further investigate the chemical states of the N of g-C_3N_4 before and after Pd deposition and the Pd on g-C_3N_4, which could help to understand the interactions between N atoms and Pd atoms [23, 29]. As shown in Fig. 4a, the N1 s core level of the g-C_3N_4 has a positive shift after Pd deposition. Fig. S1 shows that the positive shifts are about 0.1–0.3 eV for the deconvoluted peaks of N1 s. This indicates that the N

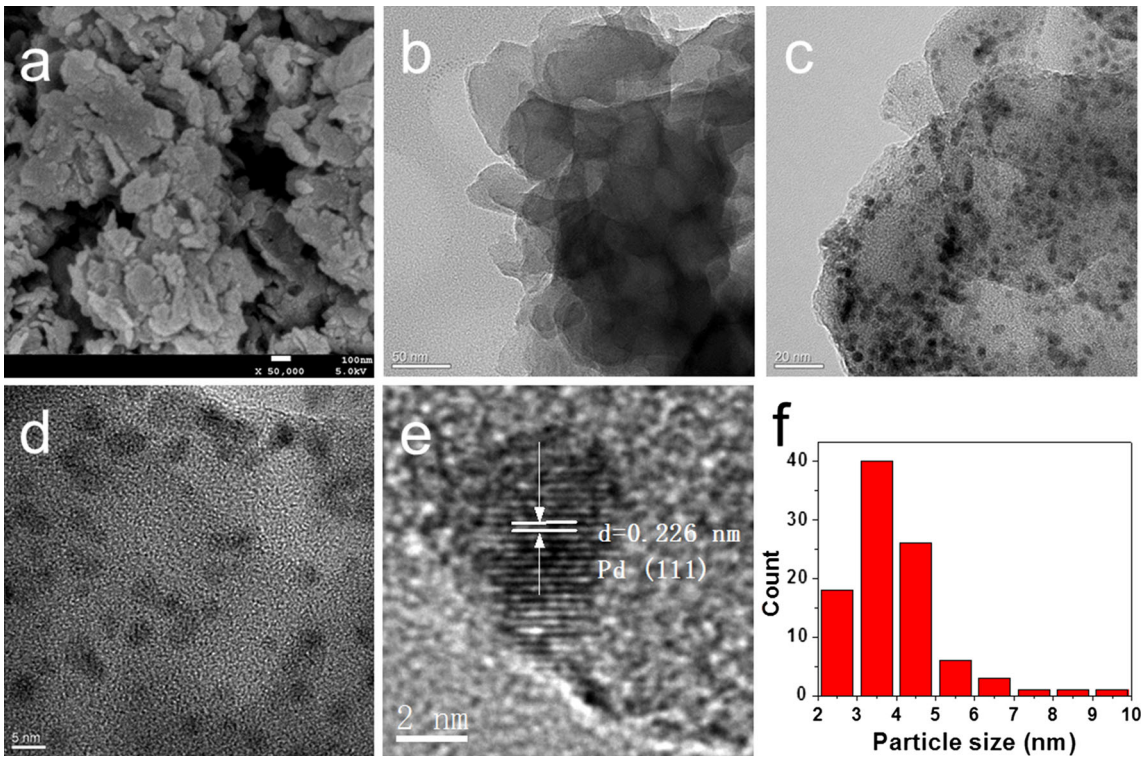

Fig. 3 SEM image of g-C_3N_4 (**a**), TEM images of g-C_3N_4 (**b**) and Pd/g-C_3N_4(**c**), HRTEM images of Pd/g-C_3N_4 (**d**, **e**) and size distribution of Pd nanoparticles (**f**)

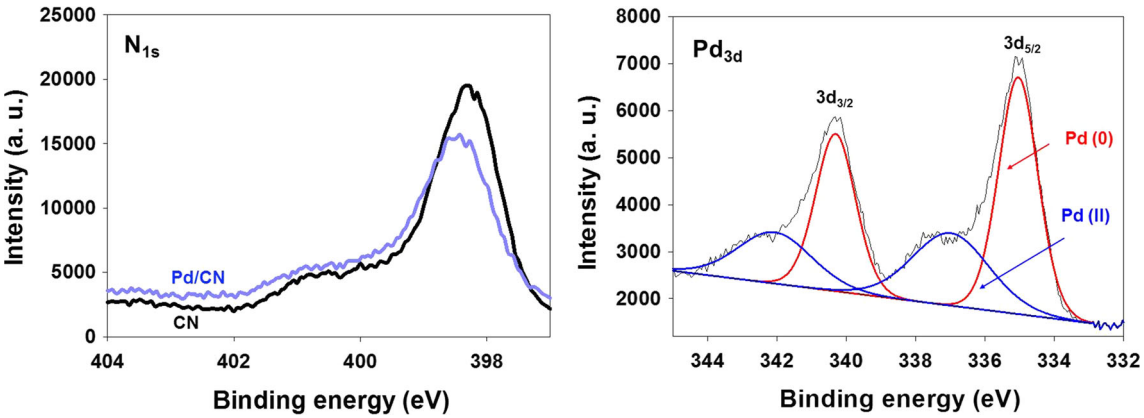

Fig. 4 XPS spectra of g-C_3N_4 and Pd/g-C_3N_4

atoms on the Pd/g-C_3N_4 are charged more positively, which may be due to the electronic transfer from the N atoms to Pd ones [23, 29]. Figure 4b illustrates the XPS spectrum of the supported Pd. There is a clear doublet that corresponds to $Pd3d_{5/2}$ and $Pd3d_{3/2}$ appeared in the spectrum. The $Pd3d_{3/2}$ peak at 340.3 eV and the $Pd3d_{5/2}$ peak at 335.0 eV are assigned to Pd(0), while the $Pd3d_{3/2}$ peak at 342.0 eV and $Pd3d_{5/2}$ peak at 337.0 eV are attributed to Pd(II) [19]. Interestingly, the peak at 335.0 eV assigned to Pd(0) is more negative than that of normal metallic palladium (335.2 eV) [30], which may be due to that the Pd nanoparticles can accept electrons from the N atoms of g-C_3N_4 [23, 29]. Furthermore, it was found that most of the surface Pd species were reduced to zerovalent form during the solution reduction. Interestingly, the Pd(II)/Pd(0) ration is about 0.71 which is much higher than that (about 0.14) for the catalyst synthesized by photodeposition [22]. Such a higher Pd(II) content may be attributed to the stronger metal-support interaction [32] which is generated during the Pd deposition. The stronger interaction would be much more beneficial to the dispersion and stability of the metallic Pd nanoparticles and the catalytic performance.

Typically, Suzuki–Miyaura reaction can be catalyzed by supported catalysts with Pd(0) and/or Pd(II) species [8, 10]. For the catalyst supported with both Pd(0) and Pd(II) species, the supported and in situ formed Pd nanoclusters are hypothesized to be the catalytic active species for the reaction [8]. To evaluate its catalytic performance and stability, the catalyst Pd/g-C_3N_4 was then tested for the Suzuki–Miyaura reactions. (Table 2). A blank reaction of iodobenzene and phenylboronic acid shows that the Suzuki–Miyaura reaction did not happen in the absence of the catalyst even after 24 h. However, to our delight, with a small amount of the catalyst (Pd, 1 mol %), iodobenzene was converted completely to the Suzuki–Miyaura product within 1 h with 99 % isolated yield. When bromobenzene was chosen as a substrate, the reaction completed smoothly in 2 h with an isolated yield of 97 %. It is worth noting that the isolated yield of the product can reach 63 % even the reaction time was 10 min. Accordingly, the TOF value for this reaction is 378 h^{-1}, which is seven times higher than the one for our previous N-free carbon-supported Pd catalyst [31]. This significant improvement of the activity can be attributable to the incorporation of N heteroatoms to the support, resulting in enhanced metal-support interaction [33]. The catalyst Pd/g-C_3N_4 was further tested in the Suzuki–Miyaura reaction of aryl halides (iodobenzene and bromobenzene) and methoxyphenylboronic acid. The results demonstrated that the catalyst exhibited high efficiency in all these reactions though the reaction times are longer than those of the reactions using phenylboronic acid as one of the two substrates. The high activity and selectivity was also found in the reactions of other aryl bromides with electron-withdrawing and donating groups and phenylboronic acid. All the reactions can be finished in the reaction time range from 2.5 to 4 h with a high isolated yield (over 95 %). However, the catalyst shows a low activity in activating aryl chloride even with longer reaction time and catalyst loading. Interestingly, the ICP analysis for the hot filtration after the reaction of bromobenzene and phenylboronic acid showed that the leaching of Pd is very little (less than 0.5 % of the total palladium). Moreover, the hot filtration from the reaction solution with about 50 % conversion showed no further reactivity at the same reaction temperature even for several hours. These results indicated the supported Pd nanoparticles may interact strongly with the support g-C_3N_4 and are very stable on the surface of the support. The remarkable stability of the

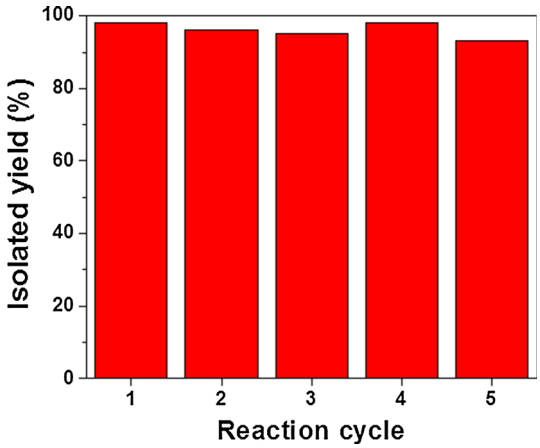

Fig. 5 Recycling of Pd/g-C_3N_4. Reaction conditions: 0.5 mmol 4-bromoanisole and 0.55 mmol phenylboronic acid, 2 mmol K_2CO_3, 4 ml H_2O-ethanol (v/v = 1:1), 80 °C for 2 h

Table 2 Suzuki-Miyaura reactions catalyzed by Pd/g-C_3N_4

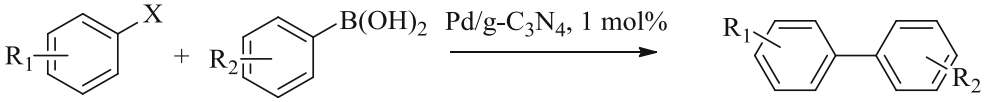

X	R_1	R_2	Reaction time (h)	Isolated yield (%)
I	4-H	H	1	99
I	4-H	4-OCH_3	2	99
Br	4-H	H	2	97
Br	4-H	4-OCH_3	3.5	97
Br[a]	4-H	H	1/6	63
Br	2-CH_3	H	4	93
Br	4-OCH_3	H	2.5	98
Br	4-CHO	H	3.5	99
Cl[b]	4-H	H	24	30

Reaction conditions: 0.5 mmol aryl halides, 0.55 mmol phenylboronic acid, 4 mg catalyst (1 mol %), 2 mmol K_2CO_3, 4 ml H_2O-ethanol (v/v = 1:1), 80 °C. The reactions were monitored by TLC

[a] The TOF is 378 h^{-1}

[b] 10 mg catalyst (2.5 mol %)

catalyst was further confirmed by the recycling experiments. It was found that the catalyst can be recycled at least for three times without any loss of activity and selectivity Fig. 5. Under the same reaction conditions, only after the fourth recycle, the isolated yield of the product decreases slightly from 98 to 93 %. The HRTEM images of the recycled catalyst revealed that overwhelming majority of the Pd nanoparticles sustain their sizes and dispersion after five reaction cycles (Fig. S2). The insignificant loss of the activity and selectivity in the fifth may be due to a small part of agglomerate Pd nanoparticles (Fig. S2). Furthermore, XPS measurement was also performed on the reused catalyst (Fig S3). As shown in Fig. S3a, there is no significant changes in peak shapes for the N1 s after reaction, which indicated that the support could be stable during the reaction. However, surprisingly, the Pd(II)/Pd(0) ratio of the reused catalyst increased to 1.5 though the chemical shifts were approximately same for the fresh and reused catalyst (Fig. S3b). During the reaction, the Pd(II) species in g-C_3N_4 might undergo a cycle of involving Pd(II) to Pd(0) by phenyl boronic acid reduction and then back to Pd(II) by oxygen oxidation [34]. The strong metal-support interaction may enhance the oxidation resulting in an increase of Pd(II) species in the used catalyst. Therefore, the results of the catalytic reactions and the recycling tests indicated that the metal-support interaction may create a highly efficient and robust catalyst for the Suzuki–Miyaura reactions.

4 Conclusions

In summary, highly uniform Pd nanoparticles with an average size of 4 nm were successfully supported on the surface of g-C_3N_4 via a solution reduction method assisted by ultrasonication. The supported Pd catalyst is highly efficient in the Suzuki–Miyaura reaction with 100 % conversion and up to 99 % isolated yield under mild reaction conditions. The results indicate that the electronic transfer from N atoms on the framework of g-C_3N_4 to Pd nanoparticles enhanced the interaction between the support and the Pd nanoparticles. It was found that the interaction is helpful for excellent dispersion and the stability of the Pd nanoparticles on the g-C_3N_4. The robust catalyst can be easily recycled for at least 4 times without Pd leaching and decline of activity and selectivity in the reaction. Although our catalyst in this paper activates aryl iodides and bromides effectively, the catalyst shows a low activity in the Suzuki–Miyaura reaction of the aryl chloride and phenylboronic acid. Our further efforts will be devoted to design new and higher active Pd-g-C_3N_4 nanocomposite which is capable of activating aryl chlorides under mild reaction conditions.

5 Supplementary Material

The Supplementary Material include the deconvoluted XPS profiles of the g-C_3N_4 before and after deposition, TEM images of the catalyst after five reaction runs and ^{1}H NRM spectra of the products.

Acknowledgments We are grateful for the financial support by the National Natural Science Foundation of China (Grant No: 20903068) and the Specialized Research Fund for the Doctoral Program of Higher Education (Grant No: 20090181120054). One of the authors A. Vinu thanks Australian Research Council for the Future Fellowship and the University of Queensland for the start-up grants. The project was also financially supported by King Saud University, Vice-Deanship of Scientific Research.

References

1. Kotha S, Lahiri K, Kashinath D (2002) Tetrahedron 58:9633–9695
2. Zapf A, Beller M (2002) Top Catal 19:101–109
3. Magano J, Dunetz JR (2011) Chem Rev 111:2177–2250
4. Alonso F, Beletskaya IP, Yus M (2008) Tetrahedron 64:3047–3101
5. Felpin FX, Ayad T, Mitra S (2006) Eur J Org Chem 12(2006):2679–2690
6. Polshettiwar V, Len C, Fihri A (2009) Coord Chem Rev 253:2599–2626
7. Ikegami S, Hamamoto H (2009) Chem Rev 109:583–593
8. Phan NTS, Van Der Sluys M, Jones CW (2006) Adv Synth Catal 348:609–679
9. Fihri A, Bouhrara M, Nekoueishahraki B, Basset J-M, Polshettiwar V (2011) Chem Soc Rev 40:5181–5203
10. Astruc D (2007) Inorg Chem 46:1884–1894
11. Borkowski T, Dobosz J, Tylus W, Trzeciak AM (2014) J Catal 319:87–94
12. Metin O, Ho SF, Alp C, Can H, Mankin MN, Gultekin MS, Chi M, Sun S (2013) Nano Research 6:10–18
13. Movahed SK, Dabiri M, Bazgir A (2014) Appl Catal A 488:265–274
14. Scheuermann GM, Rumi L, Steurer P, Bannwarth W, Muelhaupt R (2009) J Am Chem Soc 131:8262–8270
15. Ding S-Y, Gao J, Wang Q, Zhang Y, Song W-G, Su C-Y, Wang W (2011) J Am Chem Soc 133:19816–19822
16. Yuan B, Pan Y, Li Y, Yin B, Jiang H (2010) Angew Chem Int End 49:4054–4058
17. Amali AJ, Rana RK (2009) Green Chem 11:1781–1786
18. Wang Y, Wang X, Antonietti M (2012) Angew Chem Int End 51:68–89
19. Wang Y, Yao J, Li H, Su D, Antonietti M (2011) J Am Chem Soc 133:2362–2365
20. Gong Y, Li M, Li H, Wang Y (2015) Green Chem 17:715–736
21. Li X-H, Baar M, Blechert S, Antonietti M (2013) Sci Rep 3:1743–1748
22. Sun J, Fu Y, He G, Sun X, Wang X (2015) Appl Catal B 165:661–667
23. Shiraishi Y, Kofuji Y, Kanazawa S, Sakamoto H, Ichikawa S, Tanaka S, Hirai T (2014) Chem Commun 50:15255–15258
24. Lee SC, Lintang HO, Yuliati L (2012) Chem Asian J 7:2139–2144

25. Li Y, Xu X, Zhang P, Gong Y, Li H, Wang Y (2013) RSC Adv 3:10973–10982
26. Liu J, Zhang T, Wang Z, Dawson G, Chen W (2011) J Mater Chem 21:14398–14401
27. Lin Q, Li L, Liang S, Liu M, Bi J, Wu L (2015) Appl Catal B 163:135–142
28. Lu X, Xu K, Chen P, Jia K, Liu S, Wu C (2014) J Mater Chem A 2:18924–18928
29. Lee JH, Ryu J, Kim JY, Nam S-W, Han JH, Lim T-H, Gautam S, Chae KH, Yoon CW (2014) J Mater Chem A 2:9490–9495
30. Fuggle JC, Martensson N (1980) J Electron Spectrosc Relat Phenom 21:275–281
31. Zhong L, Chokkalingam A, Cha WS, Lakhi KS, Su X, Lawrence G, Vinu A (2015) Catal Today 243:195–198
32. Hoseini SJ, Heidari V, Nasrabadi H (2015) J Mol Catal A 396:90–95
33. Jiang B, Song S, Wang J, Xie Y, Chu W, Li H, Xu H, Tian C, Fu H (2014) Nano Research 7:1280–1290
34. Choi M, Lee D-H, Na K, Yu B-W, Ryoo R (2009) Angew Chem Int Ed 48:3673–3676